Acta Cryst. (1965). **18**, 609

Use of an Elastic Model in Calculating the X-ray Scattering from the Interstitial Ti-O Solid Solution

BY F. R. L. SCHOENING
Physics Department, University of Witwatersrand, Johannesburg, South Africa
AND F. WITT
The Franklin Institute Laboratories, Philadelphia, Penna., U.S.A.

(*Received* 15 *May* 1964 *and in revised form* 6 *July* 1964)

A method is described to predict and measure the static lattice distortions in titanium as produced by interstitial atoms. It is assumed that the metal can be approximated by a continuum having the elastic properties of titanium and that the interaction of the interstitial atom with the crystal lattice can be represented by a set of crossed unequal double forces which act along the principal axes of a cartesian coordinate system in the crystal. The doublets act normal to the surface of a small sphere cut out at the position where the interstitial atom is situated in the crystal and the basal plane doublets are assumed to be of equal magnitude.

The influence of thermal vibrations on the diffracted intensity has been measured both at room temperature and at liquid nitrogen temperature. The characteristic temperature, θ_m (X-ray) has been determined as a function of defect concentration.

Introduction

Many theoretical investigations of the static lattice distortions around interstitial atoms and their influence on the diffraction of X-rays have been carried out (*cf.* Ekstein, 1945; Zachariasen, 1945; Huang, 1947; Matsubara, 1952; Teltow, 1953; Cochran & Kartha, 1956; Kanzaki, 1957; Krivoglaz 1959; Flinn & Maradudin, 1962; Fisher & Hahn, 1963). The theoretical work is always based on certain models which are postulated to represent the properties of the crystal. It is the purpose of this investigation to study quantitatively the applicability of the simple elastic model. The Ti–O system was chosen because of the large interstitial solubility (33 at. %) of oxygen in titanium and because of the hexagonal symmetry of the α solid solution. Explicit solutions of the elastic problem are known for isotropic and transversely isotropic media. There being only one isotropic metal, tungsten, a hexagonal metal was an obvious choice.

The observable quantities, lattice parameter, Laue–Bragg (LB) intensity and diffuse scattering, which vary with the concentration of interstitial atoms, are not independent of each other. A model is assumed which represents the crystal, and the variation of the LB intensity with concentration can be calculated from the variation of the lattice parameter with concentration. A comparison of the calculated intensity changes with the observed intensity changes then affords a good test for the usefulness of the assumed model. Previously reported results (Schoening & Witt, 1963), although obtained by making several restrictive assumptions, indicated that such a comparison is possible and that the use of the elastic model is justifiable. In the present investigation several of the assumptions have been eliminated, and a full account of the work is given.

X-ray measurements

The experimental work was carried out at The Franklin Institute Laboratories* (FIL) in Philadelphia and at the Department of Physics in The University of the Witwatersrand (U.W.) in Johannesburg. The FIL experiments were designed to give the LB intensity as a function of oxygen concentration; the experiments at U.W.gave the ratio of the LB intensities at different temperatures for varying oxygen concentration. Some measurements at different temperatures were also done at FIL and serve as a check of the compatibility of both the FIL and U.W. results. The samples were prepared at FIL.

Sample preparation

Several monocrystals, about $0{\cdot}3\times0{\cdot}3\times0{\cdot}5$ mm in size, were prepared from large grained, zone refined (iodide) titanium. The crystals were rectangular in shape with the long faces parallel to (0001) and $(10\bar{1}0)$. The $00{\cdot}l$ and $h0{\cdot}0$ reflections were measured during rotation of the crystals around $[\bar{1}2\bar{1}0]$.

Varying amounts of oxygen were introduced into the crystals by heating in an oxygen atmosphere and, if necessary, homogenizing in vacuum afterwards. The oxygen concentration was determined from *d*-values for the $00l$ reflections using the lattice parameter published by Andersson, Collen, Kuylenstierna & Magnéli (1957). Positive and negative Bragg angles for the $00l$ and $00\bar{l}$ reflections were measured in order to minimize crystal positioning errors. Every specimen was checked for ordering of oxygen atoms by looking for the 003 reflection, which is absent for a disordered crystal. In some cases an oxide scale had formed, but

---

* Supported by AEC Contract AT(30–1)–2994.

it could easily be removed by etching and mechanical action.

Intensity measurements

A Siemens diffractometer was used at FIL and a Philips diffractometer at U.W. In both laboratories the technique of the stationary counter ($2\theta=$constant) — rotating crystal ($\omega=$variable) was employed. Before every intensity measurement, a small aperture was placed in front of the proportional counter, and the crystal was adjusted for maximum intensity. The integrated intensity measurement was made with an open counter. The total counts recorded by the scaler were corrected for background counts. No attempt was made to include the whole tail of the diffraction peaks because this would have included an undue amount of diffuse scattering intensity. In a typical run the counting was stopped when the tail intensity varied less than 1% of the peak intensity over $\frac{1}{2}°$ on the ω scale. All peaks could be recorded within an ω range of 4°.

The pronounced mosaic character of the crystals was evident. It is possible that the satellites on some of the peaks were due to influences other than mosaic structure, but this was not further investigated with the diffractometer because of its restricted scan of the reciprocal space. The mosaic structure suggested that no correction for primary extinction was necessary. In fact the low order reflections correlated well with the rest of the observations. No correction for secondary extinction was applied. There appeared to be no systematic deviation of the strong reflections from the general pattern of the results.

At U.W. the ratio of the integrated intensities at two temperatures was measured. The crystals were cooled by blowing a controlled stream of cold nitrogen gas against them. The temperature, which varied between 110 and 125 °K for different experiments, was measured by replacing the crystal with a thermistor.

At FIL instrumental fluctuations were kept at a minimum by measuring the 100 reflection after every other reflection and using the intensity ratio, and at U.W. by recording the room and low temperature intensities in close succession, keeping a long time check on the fluctuations by measuring the 002 reflection at the beginning and end of every day. Drift in the counter-amplifier–discriminator electronics was corrected, when necessary, several times a day by adjusting the counter voltage (FIL) or adjusting the discriminator window position (U.W.).

Evaluation of intensity measurements

A difficulty of principle in interpreting the recorded intensity data arises from the overlap of LB intensity and that part of the diffuse intensity which varies appreciably in the vicinity of a LB peak and is caused by the thermal and distortional diffuse scattering. The Compton modified scattering and the disorder diffuse scattering vary slowly with the scattering angle and are subtracted with the general background. The measured intensity is therefore proportional to

$$L_PA|F_o|^2e^{-2M}[1+TC_{\rm th}(\sin^2\theta)/\lambda^2+C_{\rm dis}(\sin^2\theta)/\lambda^2] \quad (1)$$

where $L_P=$Lorentz polarization factor, $A=$transmission factor, $F_o=$structure factor for the relevant oxygen concentration, $T=$ temperature in °K, $C_{\rm th}=$constant expressing thermal diffuse scattering, $C_{\rm dis}=$constant expressing distortional diffuse scattering, $M=(TB_{\rm th}+B_0+B_{\rm dis})(\sin^2\theta)/\lambda^2$ the Debye–Waller factor incorporating thermal, zero-point and distortion contributions.

In addition to simplifying assumptions made in expressing the temperature influence, the use of (1) is restricted to reflections from the same set of crystallographic planes because $C_{\rm th}$ and $C_{\rm dis}$ are taken to be constant.

Because the diffuse scattering, which is included in the integrated intensity measurements, will be small, the term in parentheses in (1) may be approximated by an exponential. The measured intensity $E(hkl)$ (counts taken during rotation of crystal through reflection) is proportional to

$$L_PA|F_o|^2\exp\{-[T(2B_{\rm th}-C_{\rm th})+2B_0+2B_{\rm dis}-C_{\rm dis}](\sin^2\theta)/\lambda^2\}\,.$$

At FIL the ratios $E(00l)/E(100)$ and $E(h00)/E(100)$ were measured. A plot of $ln\ [E(00l)/E(100)L_P(00l)A(00l)|F_o(00l)|^2]$ *vs.* $(\sin^2\theta)/\lambda^2$ has the slope

$$X(q)=-(T[2B_{\rm th}-C_{\rm th}]+2B_0+2B_{\rm dis}-C_{\rm dis})\,.$$

The parameter q, being the number of oxygen atoms in the unit cell, expresses the dependence of the slope on oxygen concentration.

In addition to the observed quantities $E(00l)$ and $E(100)$, the L_P factor, the transmission factor and the structure factor are required. The absorption correction was obtained both by the graphical method of Joel, Vera & Garaycochea (1953) and an analytical method (Witt, unpublished), the two methods agreeing within one per cent. The structure factor was calculated using atomic scattering factors with dispersion correction for titanium (Qurashi, 1954) and without dispersion correction for oxygen (Freeman, 1959). A random distribution of oxygen atoms in the octahedral interstitial sites was assumed.

At U.W. the same reflection was measured at room temperature T_1 and at low temperature T_2. A plot of $ln[E(00l, T_1)/E(00l, T_2)]$ *vs.* $(\sin^2\theta)/\lambda^2$ has the slope

$$Y(q)=-(T_1-T_2)(2B_{\rm th}-C_{\rm th})$$

Combining the FIL and U.W. data, an expression for the distortion coefficient $B_{\rm dis}$ is obtained, making use of the condition that for $q=0$, $B_{\rm dis}=0$ and $C_{\rm dis}=0$,

$$2B_{\rm dis}=[T_1/(T_1-T_2)]\,[Y(q)-Y(0)]-[X(q)-X(0)]+C_{\rm dis}\,. \quad (2)$$

In (2) the thermal diffuse scattering has been eliminated. Because of the presence of the distortional diffuse scattering, the experimental data can only give $B'_{\mathrm{dis}}=B_{\mathrm{dis}}-\frac{1}{2}C_{\mathrm{dis}}$. Either C_{dis} has to be neglected or it has to be calculated, the latter being rather difficult, if at all possible. In general, the true B_{dis} is larger than the observed B'_{dis}.

The results of the measurements of $X(q)$ and $Y(q)$ are shown in Fig. 1 and Fig. 2. The crucial comparison between the experimental B'_{dis} values, obtained from the curves in Figs. 1 and 2, and the theoretical B_{dis} values, obtained from elastic calculations and lattice parameter measurements, is shown in Fig. 3.

The $Y(q)$ data and the $X(q)$ data for 00*l* follow a definite curve, although the error attached to each individual point is large. However, X(q) for *h*00 appears to have two maxima, at 2% and 18% oxygen

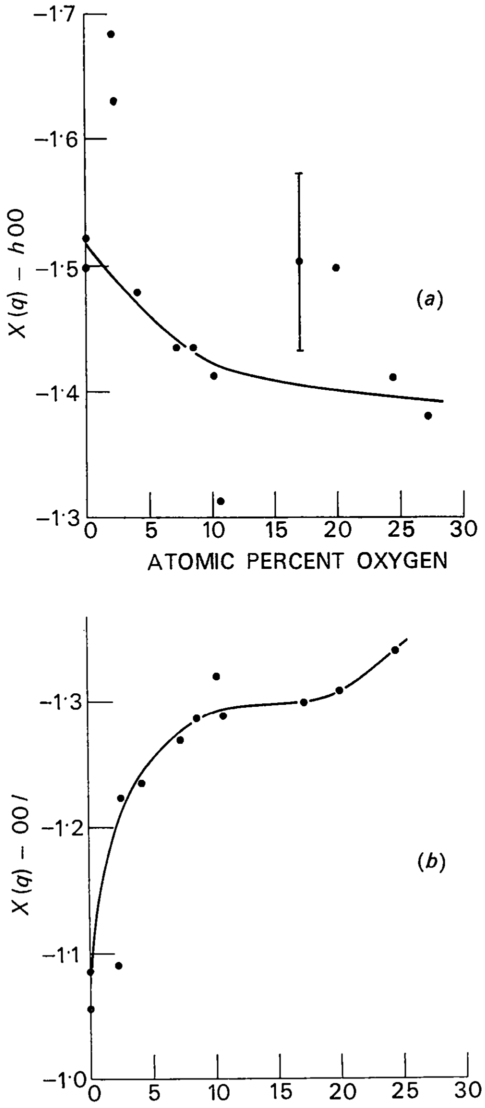

Fig. 1. (*a*) $X(q)$ for *h*00 as function of oxygen concentration. The vertical line is error for single measurement. (*b*) $X(q)$ for 00*l*.

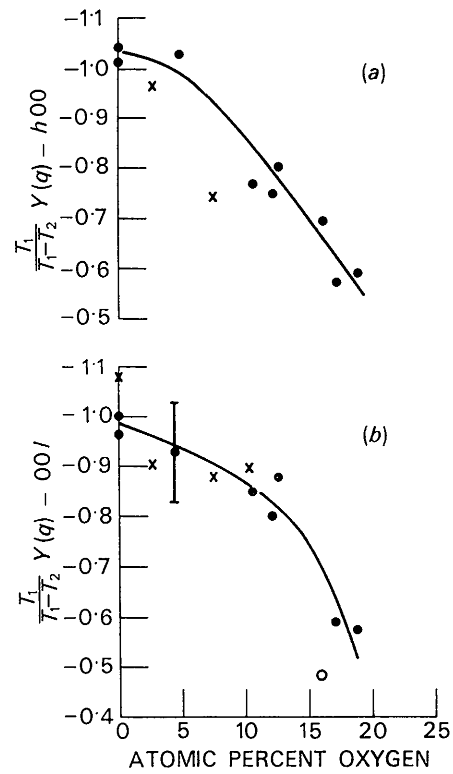

Fig. 2. (*a*) $Y(q)T_1/(T_1-T_2)$ for *h*00, (*b*) $Y(q)T_1/(T_1-T_2)$ for 00*l*. Vertical line is error for single measurement. Crosses FIL data, dots UW data, circle ordered specimen.

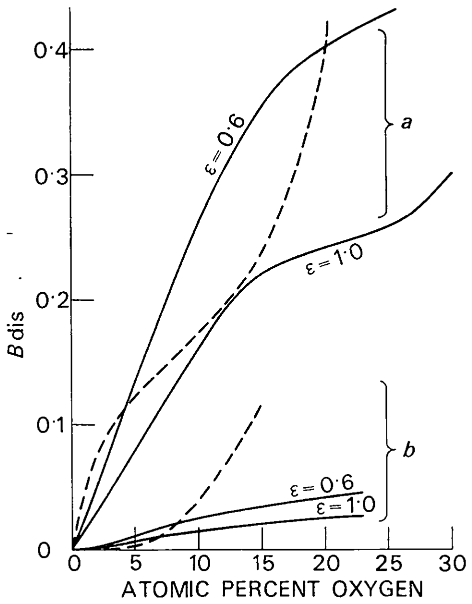

Fig. 3. Full lines are calculated B_{dis} values for cut-off radii of $\varepsilon=0{\cdot}6$ Å and 1·0 Å. Broken lines are experimental B'_{dis} data obtained from the curves in Figs. 1 and 2. (*a*) for 00*l*; (*b*) for *h*00.

concentration. In relation to the large error for each point the maxima are not very significant, but in view of the 'smooth' behavior of the 00l data, which are subject to the same errors, the maxima might indicate physical changes at these oxygen concentrations. For the purpose of calculating B'_{dis} the maxima were neglected.

Elastic calculations

The hexagonal Ti–O crystal is approximated by a transversely isotropic, elastic medium. The influence of the interstitial oxygen is replaced by pairs of opposite and equal forces, without moment, which act along the principal axis (z direction, c axis) and at right angles to it (x, y directions, in the basal plane), on the surface of a small sphere cut out at the origin, the two pairs in the xy plane being equal. The magnitude of the force pairs is adjusted to give the observed lattice parameter changes. The sum of the squares of the displacements is then calculated and finally converted to a theoretical value of B_{dis}.

Displacement field around single defect in infinite medium

The lengthy calculations can only be sketched here. The displacements in the x and z directions were obtained from Kröner (1958, 1953), the y displacement being the same as the x displacement and the P's representing the force pairs,

$$S_x = x\left[\frac{K_2}{(a_2\varrho^2+z^2)^{3/2}} + \frac{K_3}{(a_3\varrho^2+z^2)^{3/2}}\right]$$

$$S_z = -z\left[\frac{Q_2}{(a_2\varrho^2+z^2)^{3/2}} + \frac{Q_3}{(a_3\varrho^2+z^2)^{3/2}}\right] \qquad (3)$$

with

$$\begin{aligned} K_2 &= P_{xx}A_2a_2^2 + P_{zz}C_2a_2 \\ K_3 &= P_{xx}A_3a_3^2 + P_{zz}C_3a_3 \\ Q_2 &= P_{xx}C_2a_2 + P_{zz}D_2 \\ Q_3 &= P_{xx}C_3a_3 + P_{zz}D_3 \\ \varrho^2 &= x^2+y^2\,. \end{aligned}$$

The A_i, C_i, D_i and a_i which are functions of the elastic moduli for titanium ($s_{11}=0{\cdot}949$, $s_{33}=0{\cdot}667$, $s_{44}=2{\cdot}146$, $s_{12}=-0{\cdot}480$ and $s_{13}=-0{\cdot}162\times10^{12}$ cm^{2}dyne^{-1}, become

$$\begin{aligned} K_2 &= -P_{xx}3{\cdot}162\times10^{22} + P_{zz}4{\cdot}087\times10^{22} \\ K_3 &= P_{xx}1{\cdot}517\times10^{22} - P_{zz}1{\cdot}063\times10^{22} \\ Q_2 &= P_{xx}4{\cdot}087\times10^{22} - P_{zz}5{\cdot}279\times10^{22} \\ Q_3 &= -P_{xx}1{\cdot}063\times10^{22} + P_{zz}0{\cdot}742\times10^{22} \\ a_2 &= 2{\cdot}060 \\ a_3 &= 0{\cdot}536\,, \end{aligned}$$

all units being in the c.g.s. system.

The P's were found by equating the observed volume expansions ΔV_x^∞ and ΔV_z^∞ to the expansions calculated from the x and z displacements respectively. Using the observed lattice parameters,

$$\int \mathbf{S}_{\mathrm{x}}\,.\,\mathbf{n}dA = \Delta V_x^\infty = \frac{V_c}{q\gamma}\frac{\Delta a}{a} \qquad (4)$$

similarly for ΔV_z^∞, and where the integral is taken over a sphere with normal $\mathbf{n}$ and surface element dA, V_c is the cell volume, q is the number of oxygen atoms in the cell and γ is a parameter which compensates for the image effects and is unity for an infinite crystal (Eshelby, 1956). The lattice parameter data (Andersson *et al.* 1957) which have been used in (4) show that Δa and Δc are not linear functions of the oxygen concentration. This means that the forces exerted by a single defect change with oxygen concentration, indicating possible interaction between defects at higher concentrations.

Eliminating the P's in this way leads to

$$\begin{aligned} K_2 &= -0{\cdot}1814\,\Delta V_x^\infty + 0{\cdot}3606\,\Delta V_z^\infty \\ K_3 &= 0{\cdot}1515\,\Delta V_x^\infty - 0{\cdot}0690\,\Delta V_z^\infty \\ Q_2 &= 0{\cdot}2341\,\Delta V_x^\infty - 0{\cdot}4644\,\Delta V_z^\infty \\ Q_3 &= -0{\cdot}1072\,\Delta V_x^\infty + 0{\cdot}0496\,\Delta V_z^\infty\,. \end{aligned} \qquad (5)$$

The theoretical B_{dis} has to be obtained from the volume integrals $\int S_x^2 dV$ and $\int S_z^2 dV$; introducing a cut-off radius ε for the purpose of excluding the origin, the integrals become respectively,

$$(2\pi/\varepsilon)\,[0{\cdot}1206\,K_2^2 + 3{\cdot}0139\,K_3^2 + 1{\cdot}0972\,K_2K_3] \text{ and}$$
$$(4\pi/\varepsilon)\,[0{\cdot}1567\,Q_2^2 + 0{\cdot}7322\,Q_3^2 + 0{\cdot}5866\,Q_2Q_3]\,.$$

The dependence on oxygen concentration follows from (5) and (4).

Finite crystal, image effects

The influence of image forces was estimated by constructing an isotropic medium with average elastic constants and using Eshelby's (1956) results for this case. The average elastic constants were calculated according to Leibfried (1953) and are $\bar{c}_{11}=1{\cdot}64\times10^{12}$ and K (bulk modulus)$=3{\cdot}12\times10^{12}$. Eshelby (1956) gives $\Delta V = \Delta V^\infty + \Delta V^I = \gamma\Delta V^\infty$ where $\gamma = K/\bar{c}_{11}$ and ΔV, ΔV^∞ and ΔV^I are the total, the infinite medium and the image force expansions, respectively. The value of $\gamma=1{\cdot}9$ was used in (4).

Effect of displacement field on Laue-Bragg intensities

The influence of static lattice distortions on the LB intensities is expressed by the factor $\exp\{-2B_{\mathrm{dis}}(\sin^2\theta)/\lambda^2,\}$ where $B_{\mathrm{dis}}=8\pi^2\overline{\Delta^2}$ and $\overline{\Delta^2}$ is the mean square displacement from the average lattice. It is assumed that the mean square displacements are the same for Ti and O atoms, and that they follow a normal distribution. Krivoglaz (1959) showed that for large distortions and for large values of $(\sin^2\theta)/\lambda^2$, $\overline{\Delta^2}$ may be in error by 30%. The deviation from the normal distribution results in a non-linear plot of log-intensity *vs.* $(\sin^2\theta)/\lambda^2$ and in different 'slopes' of these plots for different directions of the normals of the diffracting planes. Because in Ti–O the displacements are small and the experimental uncertainty is too large to show non-linearity in the log *I* plots, the simple exponential factor was used.

Following Cochran & Kartha (1956) and introducing the displacement components $\overline{\Delta_c^2}$ and $\overline{\Delta_a^2}$ for *z* and *x* directions respectively, it follows that $\overline{\Delta_c^2}=n\overline{\Delta_{1c}^2}=(n/N)\Sigma\Delta_{1c}^2=q\Sigma\Delta_{1c}^2$ where *n* is the number of defects, *N* is the number of unit cells and Δ_{1c} is the displacement caused by one defect. Taking into consideration the image displacement δ_c^i it is $\Delta_{1c}=\delta_c^\infty+\delta_c^i-\delta_c$ (hom), where δ_c^∞ is the displacement which one defect would cause in an infinite crystal and δ_c(hom) is the displacement which can be expressed as a homogeneous strain.

The results of Eshelby (1956) suggest that δ_c^i is a uniform expansion; hence $\delta_c(\text{hom})=\delta_c^i+\delta_c^\infty(\text{hom})$. Because the specimen is large in comparison to the extent of the displacement field around the defect (except for defects near the surface), $\delta_c^\infty(\text{hom})=0$, which gives $\Delta_{1c}=\delta_c^\infty$, and finally,

$$B_{\text{dis}}=8\pi^2q\Sigma S_z^2, \qquad \text{where} \qquad \delta_c^\infty=S_z\,.$$

A similar equation is valid for S_x. The sum over all cells was replaced by the integral $V_c^{-1}\int S_z^2dV$ over the volume of the crystal, V_c being the unit cell volume. In Fig. 3, the resulting B_{dis} is shown as a function of the oxygen concentration and for cut-off radii of 1 Å and 0·6 Å, which is the oxygen radius.

Debye temperature

An estimate of the Debye temperature was obtained by assuming that the thermal diffuse scattering which is included in the measured intensities is negligible. It was estimated that the maximum thermal contribution was not more than 1·5% (Annaka, 1962). Hence,

$$2B_{\text{th}}=C_{\text{th}}-Y(q)/(T_1-T_2) \quad \text{or} \quad 2B'_{th}=-Y(q)/(T_1-T_2)$$

when neglecting C_{th}.

Following Zener (1936), two temperatures can be defined for the 00*l* and *h*00 reflections, respectively. In Fig. 4 are shown the formal values for the equivalent Debye temperature obtained from Fig. 2 and

$$B'_{th}=8\pi^2\{\beta-\gamma/T_1T_2+\delta(1/T_1^3-1/T_2^3)/(T_1-T_2)\}$$

(*cf.* James, 1958).

The Debye temperature for zero oxygen concentration can be compared with the equivalent Debye temperature of 351 °K for measurements made at 200 °K obtained from Garland & Slutzky (1958), who used specific heat data by Kothen & Johnston (1953). Debye temperatures of 404 and 394 °K for 0 °K were calculated from the elastic constants using methods of Anderson (1963) and Wolcott (1959), respectively. Kaufman (1961) has calculated the Debye temperature by using the empirical Lindemann melting point formula and obtained 365 °K for no oxygen, 400 °K for 5·8% oxygen and 493 °K for 25% oxygen.

Discussion

The applicability of the elastic model and of the simple exponential factor $\exp\{-16\pi^2\overline{\Delta^2}\,(\sin^2\theta)/\lambda^2\}$ may be judged from Fig. 3. The theoretical B_{dis} curve depends largely on the value taken for the cut-off radius which should be close to the oxygen radius of 0·6 Å. The experimental values lie near the curves for $\varepsilon=1$ and $\varepsilon=0{\cdot}6$ Å. Considering that the true experimental B_{dis} would be somewhat higher than the B'_{dis} shown, the use of the simple elastic model gives a reasonable result. Above 15% for 00*l* and 10% for *h*00, the experimental and calculated curves are divergent, indicating a breakdown of the model.

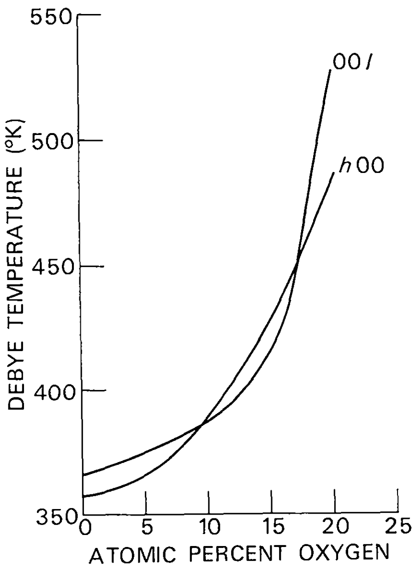

Fig. 4. Debye temperature as a function of oxygen concentration.

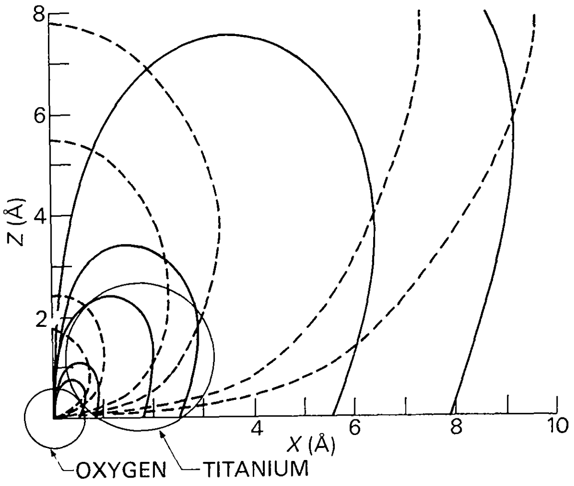

Fig. 5. *X* displacement (full lines) and *Z* displacement (broken lines) around interstitial oxygen at origin. Starting at origin the displacements are 0·1, 0·05, 0·01, 0·005, 0·001 and 0·0005 Å, respectively.

For 10% oxygen the displacement field has been calculated from (3) and (5) for a single defect and is shown in Fig. 5. This field, when linearly superimposed with $n-1$ similar fields gives the correct lattice expansion for 10% oxygen or n defects. The displacements are small, about 0·015 Å at the position of the nearest Ti atoms. In the vicinity of the interstitial oxygen they are obviously unrealistic considering the rapid variation of the displacement within the volume of the Ti atom. It may be concluded that the detailed features of the displacement field have no physical basis. Its merit lies in the fact that it gives the correct lattice expansion and the right order of magnitude for the LB intensity reduction. Other physically more satisfying models may do the same. However, by using a similar elastic model it is possible to estimate the defect concentration for other systems by measuring the lattice parameter and intensity changes. The Ti–O results show that the right order of magnitude for the concentration can be obtained in this manner.

The authors wish to thank Mr. W. Benner for his help in collecting X-ray data at FIL.

References

ANDERSON, O. L. (1963). *Phys. Chem. Solids,* **24**, 909.

ANDERSSON, S., COLLEN, B., KUYLENSTIERNA, U. & MAGNÉLI, A. (1957). *Acta Chem. Scand.* **11**, 1641.

ANNAKA, S. (1962). *J. Phys. Soc. Japan,* **17**, 846.

COCHRAN, W. & KARTHA, G. (1956). *Acta Cryst.* **9**, 944.

EKSTEIN, M. G. (1945). *Phys. Rev.* **68**, 120.

ESHELBY, J. D. (1956). *Solid State Physics,* **3**, 79.

FISHER, K. & HAHN, H. (1963). *Z. Phys.* **172**, 172.

FLINN, P. A. & MARADUDIN, A. A. (1962). *Ann. Physics,* **18**, 81.

FREEMAN, A. J. (1959). *Acta Cryst.* **12**, 261.

GARLAND, C. W. & SLUTZKY, L. J. (1958). *J. Chem. Phys.* **28**, 331.

HUANG, K. (1947). *Proc. Roy. Soc.* A, **190**, 102.

JAMES, R. W. (1958). *The Optical Principles of the Diffraction of X-Rays,* p. 237. London: Bell.

JOEL, N., VERA, R. & GARAYCHOCHEA, I. (1953). *Acta Cryst.* **6**, 465.

KANZAKI, H. (1957). *Phys. Chem. Solids,* **2**, 24, 107.

KAUFMAN, L. (1961). ASD Technical Report 61-445.

KOTHEN, C. W. & JOHNSTON, H. L. (1953). *J. Amer. Chem. Soc.* **75**, 3101.

KRIVOGLAZ, M. A. (1959). *Fiz. Metal. Metalloved.* **7**, 650.

KRÖNER, E. (1953). *Z. Phys.* **136**, 402.

KRÖNER, E. (1958). *Kontinuumstheorie der Versetzungen und Eigenspannungen, Ergebnisse der Angewandten Mathematic.* Vol. 5. Berlin: Springer.

LEIBFRIED, G. (1953). *Z. Phys.* **135**, 23.

MATSUBARA, T. (1952). *J. Phys. Soc. Japan,* **7**, 270.

QURASHI, M. M. (1954). *Acta Cryst.* **7**, 310.

SCHOENING, F. R. L. & WITT, F. (1963). *Advanc. X-Ray Analysis,* **6**, 136. (W. M. MUELLER & M. FAY, Editors). New York: Plenum Press.

TELTOW, J. (1953). *Ann. Phys. Lpz.* **12**, 111.

WOLCOTT, N. M. (1959). *J. Chem. Phys.* **31**, 536.

ZACHARIASEN, W. H. (1945). *Theory of X-Ray Diffraction in Crystals.* New York: Wiley.

ZENER, C. (1936). *Phys. Rev.* **49**, 122.

Acta Cryst. (1965). **18**, 614

The Crystal and Molecular Structure of $Fe(CO)_3(C_6H_5C_2C_6H_5)_2$

BY R. P. DODGE AND V. SCHOMAKER

Union Carbide Research Institute, P. O. Box 278, Tarrytown, New York, U.S.A.

(*Received* 24 *April* 1964 *and in revised form* 25 *June* 1964)

A single-crystal X-ray diffraction study of $Fe(CO)_3(C_6H_5C_2C_6H_5)_2$ has shown it to be tetraphenylcyclobutadiene iron tricarbonyl. The final refined structure shows the cyclobutadiene ring to be square planar with ring-bond distance 1·46 Å.

Introduction

The yellow crystalline substance $Fe(CO)_3(C_6H_5C_2C_6H_5)_2$, one of a series of "tolane iron carbonyl complexes", was prepared and studied by Hübel, Braye, Clauss, Weiss, Krüerke, Brown, King & Hoogzand (1959). This product of the reaction of $Fe(CO)_5$ and diphenylacetylene was found to be stable at the melting point (234 °C) in contrast to other compounds in this series. Reductive degradation indicated that the two tolane molecules do not form separate ligands.

One of the anticipated structures was that of tetraphenylcyclobutadiene iron tricarbonyl and this possibility was confirmed by X-ray diffraction. The preliminary results were the subject of an earlier note (Dodge & Schomaker, 1960). The present paper is a presentation of the complete results from least-squares refinement.

Experimental

The crystal used, a flat square plate approximately 200 μ on a side and 60 μ thick, was selected from a sample suppled by Dr. Hübel.

A zirconium-filtered Mo $K\alpha$ source was used to collect a total of 2204 independent reflections, of which